Compression-Induced Structural Transition in a Self-Assembled Monolayer

Kenneth J. Tupper* and Donald W. Brenner

Chemistry Division, Code 6179, Naval Research Laboratory, Washington, DC 20375-5342

Molecular dynamics simulations are used to probe the atomic-scale behavior of a model for a self-assembled monolayer of *n*-hexadecanethiol chemisorbed on a gold (111) surface compressed under high loads. These simulations suggest that SAMs may undergo abrupt rearrangements during compression that retain efficient packings of the chains. These changes may in turn modify the elastic properties of the films without chain entanglement or film destruction. We propose that the signature of such a transition is visible in a force profile recently measured by Joyce *et al.* (*Phys. Rev. Lett.* **1992,** *68,* 2790) with an interfacial force microscope.

New techniques such as the Surface Force Apparatus,[1] Atomic-Force Microscope,[2] and Interfacial-Force Microscope (IFM)[3] are providing tremendous new insights into molecular behavior at the atomic scale. These insights in turn are beginning to provide a basis for designing new materials from the molecular level up. Because this is a new regime in materials science, however, there remains new and unexpected behavior that is often difficult to interpret in these experiments. It is in this area that atomistic computer simulations provide a powerful, and in some cases essential, tool for understanding material properties.[4]

In this work, molecular dynamics simulations have been used to probe the atomic-scale behavior of a model for a self-assembled monolayer (SAM) of *n*-hexadecanethiol chemisorbed on a gold (111) surface compressed to high loads. The simulations predict a compression-induced structural transition involving an abrupt change in packing of the chains. This transition separates two regimes where the response of the film to compression differs. Analysis of structure factors indicates that both structures are ordered, but with a different two-dimensional packing of the head groups. We propose that the signature of this transition is visible in an experimental force profile recently measured during loading with an IFM.[3]

The model used for the monolayer film and the monolayer-to-surface interactions is based on a model developed by Hautman and Klein.[5] Each chain is composed of pseudoatoms representing the groups CH_2, CH_3, and the sulfur head groups. Intrachain forces due to bond bending are modeled using harmonic potential energy expressions while torsional motion is modeled using a series expansion in the cosine of the dihedral angle. Interchain forces are modeled using pair-additive Lennard–Jones 12-6 potentials. In the orginal model proposed by Hautman and Klein, intramolecular bonds are held rigid, and the surface is modeled as a continuum interacting with the pseudoatoms via a 12-3 potential.[5] Because of the possibility of greatly distorting the films under high compression, these

Table 1. Potential Functions and Parameters for the Intrachain Stretching Interactions and Chain-to-Surface Interactions

$$U_{\text{stretch}}(r) = \frac{k}{2}(r - r^e)^2$$

$k_{CH_2-CH_3} = 27.38$ eV/Å^2	$k_{CH_2-CH_2} = 27.38$ eV/Å^2	$k_{CH_2-S} = 20.00$ eV/Å^2
$r^e_{CH_2-CH_3} = 1.523$ Å	$r^e_{CH_2-CH_2} = 1.523$ Å	$r^e_{CH_2-S} = 1.815$ Å

$$U_{\text{chain-surface}}(r) = 2.117\epsilon\left[\left(\frac{\sigma}{r}\right)^{12} - \left(\frac{\sigma}{r}\right)^{3}\right]$$

$\epsilon_{Au-CH_3} = 6.20 \times 10^{-3}$ eV	$\epsilon_{Au-CH_2} = 4.48 \times 10^{-3}$ eV	$\epsilon_{Au-S} = 1.75 \times 10^{-1}$ eV
$\sigma_{Au-CH_3} = 3.495$ Å	$\sigma_{Au-CH_2} = 3.495$ Å	$\sigma_{Au-S} = 2.565$ Å

two aspects of the model were changed for these simulations. First, the constraint of rigid intrachain bonds was replaced by a harmonic potential with a force constant taken from molecular mechanics[6] (see Table 1). The average bond distance decreased by 0.05 Å at our highest compression (see below), suggesting that this modification is necessary for this study. Second, the flat surface was replaced with discrete surface atoms interacting with the chain pseudoatoms via a sum of 12-3 potentials. The parameters were fit to give an interaction energy with the surface and a surface-to-head group distance that was comparable to that given by the continuum approximation[5] (see Table 1). For a single chain interacting with the surface, the continuum model gives a binding energy of 1.21 eV, while the explicit surface atom model used in this study gives a binding energy of 1.28 eV. Both models give a surface-to-head group distance of 2.41 Å. It should be noted that the surface is simulated in these studies as a single rigid layer of atoms, and that the intent of this modification is to anchor the chains laterally to the surface.

The simulated monolayer is composed of 64 chains in a supercell containing 192 gold substrate atoms. A two-dimensional infinite (111) surface is modeled using periodic boundaries. At the minimum-energy density, the sulfur head groups bind at the three-fold hollow surface sites (in agreement with recent *ab initio* calculations[7]) and form a hexagonal lattice with a nearest-neighbor spacing of 4.99 Å that is commensurate with the surface. The chains have a tilt angle (as measured from the surface normal) of 28°. These properties agree with experimental observations under ambient conditions.[8] The dynamics

* Abstract published in *Advance ACS Abstracts,* June 15, 1994.

(1) Israelachvili, J. *Intermolecular and Surface Forces*; Academic Press: San Diego, 1985.

(2) Burnham, N. A.; Colton, R. J. In *Scanning Tunneling Microscopy and Spectroscopy*; Bonnell, D., Ed.; VCH: New York, 1993; p 191, and references therein.

(3) Joyce, S. A.; Thomas, R. C.; Houston, J. E.; Michalske, T. A.; Crooks, R. M. *Phys. Rev. Lett.* **1992,** *68,* 2790.

(4) Landmann, U.; Luedtke, W. D.; Burnham, N. A.; Colton, R. J. *Science* **1990,** *248,* 454; see also *Mater. Res. Soc. Bull.* **1993,** *18.*

(5) Hautman, J.; Klein, M. L. *J. Chem. Phys.* **1989,** *91,* 4994; **1990,** *93,* 7483.

(6) Allinger, N. L. *J. Am. Chem. Soc.* **1977,** *99,* 8127.

(7) Ulman, A. *An Introduction to Ultrathin Organic Films*; Academic Press: Boston, 1991; p 289.

(8) Camillone, N., III; Chidsey, C. E. D.; Eisenberger, P.; Fenter, P.; Li, J.; Liang, K. S.; Liu, G.-Y.; Scoles, G. *J. Chem. Phys.* **1993,** *99,* 744 and references therein.

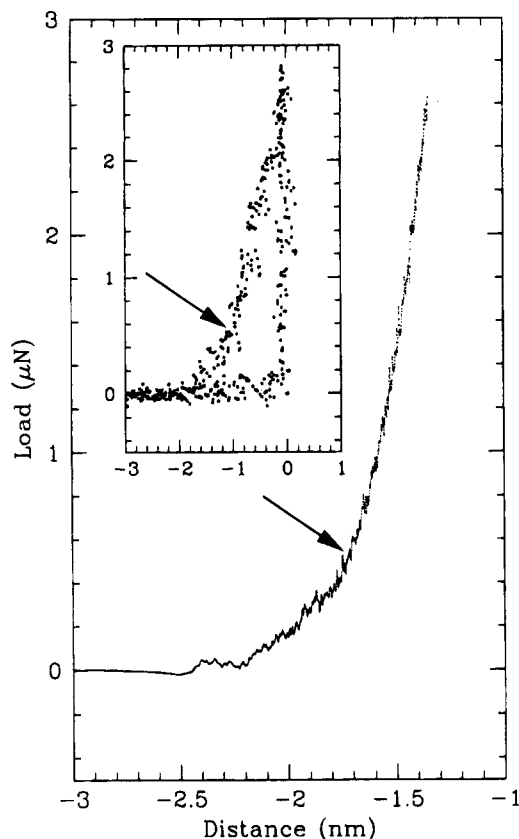© 1994 American Chemical Society

Figure 1. Calculated load on the top rigid layer versus distance between the top and bottom gold layers. Inset: Experimental data measured using the IFM described in ref 2 (from J. E. Houston). The arrows indicate the inflection points in the data curves.

were calculated by integrating classical equations of motion using a velocity Verlet algorithm[9] with a constant step size of 0.25 fs. Room temperature was maintained by scaling the atomic velocities every 20 timesteps. Before compression, the monolayer film was annealed for 50 ps. Monitoring of the tilt angle, energy, and relative orientation of the chains indicated that equilibrium was attained.

After equilibration, the film was compressed by moving a flat (111) gold surface containing 192 atoms toward the substrate at a constant velocity of 1 Å/ps. This configuration represents compression with an infinitely large flat surface, or compression with a tip whose contact area is large compared to the area of our supercell (as in the experimental IFM study of Joyce et al. discussed below). Figure 1 illustrates the simulated force profile (SFP) calculated by adding the forces on the top surface in the direction of compression.[10] The force has been converted to correspond to the experimental force profile (EFP) recently reported by Joyce et al.[3] by multiplying the force per chain in the simulation by the ratio of the experimental contact area (78.54 nm^2) to the area per molecule (0.214 nm^2). At the initial indentation, the SFP is approximately linear up to a distance of ≈1.8 nm between the gold surfaces. This region involves a uniform change in tilt angle, with little other distortion of the film in agreement with recent Monte Carlo simulations.[11] The molecular dynamics simulations predict, however, that compression beyond ≈1.8 nm results in a marked change in the response

of the film as indicated by the increase in slope in the SFP. The tilt angle in this region continues to increase uniformly with no change in slope suggesting that some other factor is responsible for the change in compressibility. Analysis of structures for the sulfur head groups of the film (see below) shows that this change in response is due to a structural transition involving an abrupt change in packing of the chains.

Recently, Joyce et al. studied the mechanical relaxation of a SAM of n-hexadecanethiol adsorbed on a gold substrate using an IFM.[3] Their data, reproduced as the inset in Figure 1, indicate several regions where the mechanical response of the film to compression differs. After initial contact, the EFP first increases with an approximately linear slope. At the highest compression, the slope of the EFP corresponds to the compression of the bare substrate. It is important to note that adhesion between the tip and the substrate was not observed during the experiment. Removing the load from the highest compression produced a large hysteresis in the EFP which Joyce et at. attribute to chain entanglement. Siepmann and McDonald, however, have pointed out that the change in energy at the full compression given in the data of Joyce et al. corresponds to approximately 20 times the binding energy of the film, which "implies that very substantial structural rearrangement must have occurred within the monolayer, and this well could have had the effect of destroying it".[11] They have also pointed out that at an intermediate compression of ≈1.4 nm, the film shows a change in mechanical response as indicated by an increase in slope in the EFP during compression. The origin of this change, however, and its relationship to the hysteresis during unloading remains unclear from these two studies. On the basis of the simulations reported here, we propose that the change in slope in the EFP during compression at ≈1.4 nm is not due to chain entanglement or destruction, but rather is due to an abrupt load-induced change in the packing of the chains that alters the elastic properties of the film.[12] Because this change involves only an ordered repacking of the chains and is visible on the relatively short timescale of the simulation, it is not related to the hysteresis which involves processes with measured relaxation times of approximately 0.04 s. This is supported by the experimental observation that the magnitude of the hysteresis decreases as the speed of the experimental indentation increases.[3,13]

To relate the change in elastic properties of the simulated film with a structural transition, structure factors S in the surface plane for the head groups as a function of load were calculated in the simulations using the expression

$$S(\mathbf{Q}) = \left| \frac{1}{N}\sum_{j=1}^{N} e^{(i\mathbf{Q}\cdot\mathbf{R}_j)} \right|^2 \qquad (1)$$

The quantity $\mathbf{Q}$ is a reciprocal lattice vector given as a multiple of 2π over the box length, $\mathbf{R}_j$ are the components of the positions in the plane of the surface of the sulfur head groups, and the sum is over all of the chain head groups. The resulting structure factors at distances of 1.95 and 1.40 nm for the SFP in Figure 1 are given in Figures 2, parts a and b, respectively. The difference in peak positions indicates a change in structure for the head

(9) Verlet, L. *Phys. Rev. B* **1967**, *159*, 98.

(10) The force curve can also be estimated by taking the numerical derivative of the total energy, including heat loss due to velocity rescaling, with respect to the change in volume. This results in the same curve as that shown in Figure 1.

(11) Siepmann, J. I.; McDonald, I. R. *Phys. Rev. Lett.* **1993**, *70*, 453.

(12) The distances reported in the SFP are the separation between the two gold surfaces. For the EFP, the distances are scaled to where the force begins to increase significantly. Assuming a value of 0.4 nm for the distance taken up by the film on the surface at full compression—a reasonable value—brings the estimated distance of the inflection point in the EFP into agreement with that observed in the SFP.
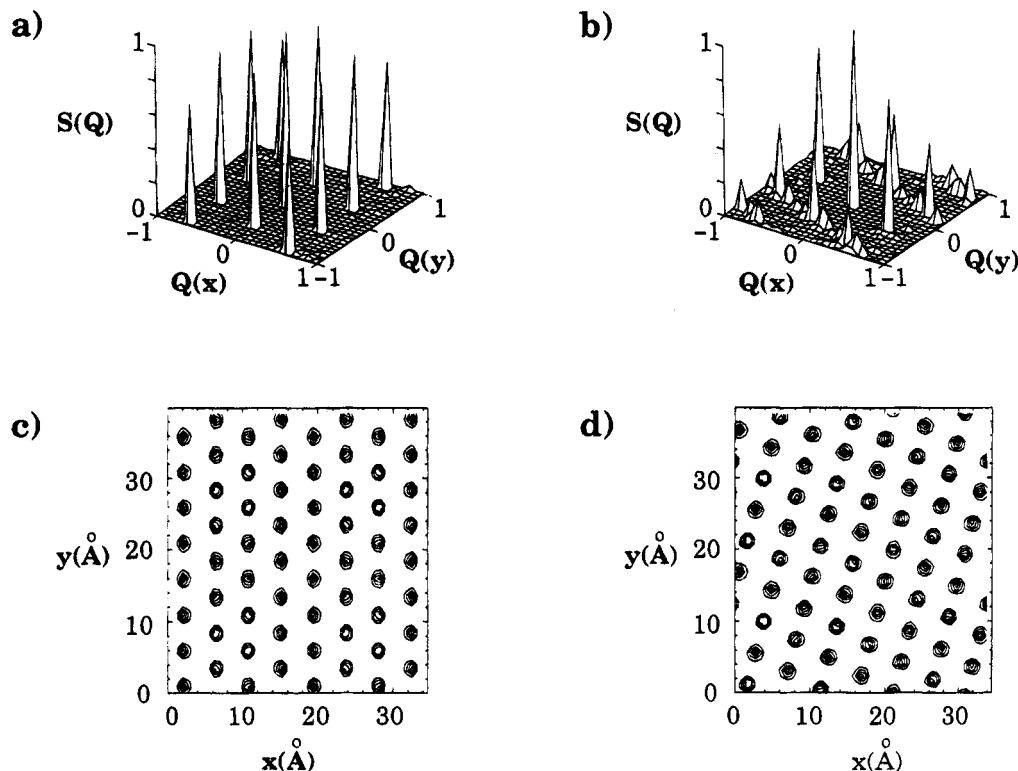
(13) Houston, J. E., private communication.

Figure 2. Calculated structure factors and real space images of the head groups. (a) Structure factors at a distance of 1.95 nm (load of 0.18 μN). (b) Structure factors at a distance of 1.40 nm (load of 1.80 μN). (c) Real space image at a distance of 1.95 nm calculated by Fourier transforming the structure factors in a. (d) Real space image at a distance of 1.40 nm calculated by Fourier transforming the 11 major peaks in b.

groups. The sharp peaks in both regimes suggest that the head groups remain ordered both at high and low compression. The secondary peaks in the highly compressed region, however, suggest a defected structure, in agreement with real-space images of the simulated head groups. Figure 3a shows the sum of the heights of the major peaks in the structure factors that are not shared by the two structures as a function of compression. The loss of the initial structure occurs between 1.9 and 1.8 nm, with the new structure growing in as the transition progresses. The change in slope of the SFP corresponds with the loss of the first structure, while the increasing slope corresponds to the formation of the new structure. Distinct peaks also occur in the structure factors of other atoms within the chains including the CH_3 tail groups, suggesting that the chains remain reasonably ordered throughout the compression.

To extract the underlying two-dimensional crystal structures for the head groups, the 12 major peaks in the structure factors were back transformed into real space giving the lattices illustrated in Figures 2, parts c and d. The two-dimensional lattice apparently goes from a hexagonal to oblique structure during the transformation, with ≈50% of the head groups going from three-fold hollow to approximately bridge sites on the substrate. Annealing of the system for an additional 5 ps at the highest compression resulted in a large decrease in the intensity of the secondary peaks in the structure factors, with relatively little change in the primary peaks. This indicates a decrease in the number of defects and that the head groups remain ordered. Annealing for an additional 5 ps yielded no other changes in the structure factors.

Illustrated in Figure 3b are the contributions from various terms in the potential function to the total potential energy of the film as a function of compression. The structural transition occurs as the potential energy
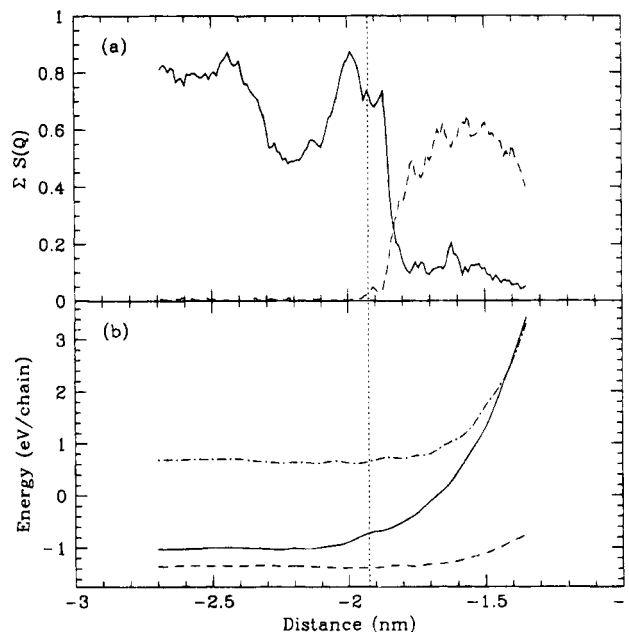
Figure 3. (a) Sum of the structure factors for the six major peaks in Figure 2, parts a and b, not shared by the two structures. Solid line: hexagonal head group structure; Dashed line: oblique head group structure. (b) Various contributions to the potential energy as a function of distance between the rigid surfaces. Solid line: interchain interactions; dashed line: chain–surface interactions; dot–dash line: intrachain interactions. The vertical dotted line depicts the initial formation of the oblique head group structure and a change in slope in the interchain interactions.

due to the interchain Lennard–Jones interactions increases, with the other contributions remaining relatively constant during the transition. Apparently the primary forces contributing to the transition are from the interchain interactions. Further support for this assertion is a subtle

decrease in the slope of the interchain potential energy with respect to compression when the structure factors for the high-load phase begin to appear (marked by the vertical dotted line in Figure 3b).

The origin of the transition can be understood by considering the interplay between the chain and head-group packings and the tilt angle. Before a load is applied, the head groups form a two-dimensional close-packed structure. As mentioned above, in this structure each headgroup occupies a three-fold hollow site, and the overlayer has a $\sqrt{3} \times \sqrt{3}$ $R30°$ structure relative to the gold substrate atoms. This spacing, however, does not correspond to a close-packed structure for the chains when they are arranged normal to the surface; this causes the chains to tilt relative to the surface normal. When viewed down the chains, the chain packing (with the 28° tilt angle) also appears approximately close packed, but with a smaller lattice constant than the head groups. Upon initial compression, the average tilt angle increases, and the close-packed structure of the chains is distorted. This destabilizes the chain−chain interactions. At the transition, a further rapid destabilization of the interchain energetics is delayed by the rearrangement of the chains back to an approximately close-packed structure, but one with a larger tilt angle and smaller lattice constant relative to the uncompressed film. This abrupt change in packing of the chains occurs at the expense of forming the oblique structure in the surface plane for the head groups. We note, however, that the chain to surface potential energy contribution remains negative throughout the compression, even after the total potential energy for the film becomes positive. This is consistent with the films remaining between the tip and substrate at high loads observed in the IFM experiment.

In conclusion, the simulations reported here on our model system suggest that SAMs may undergo abrupt rearrangements during compression that retain efficient packings of the chains. These changes may in turn modify the elastic properties of the films without chain entanglement or film destruction. Precedence for this conclusion comes from a similar change in elasticity due to a compression-induced first-order phase transition for a physisorbed surfactant monolayer on mica in saturated decane vapor observed using an SFA.[14] On the basis of the results presented here and their correlation with the IFM experiments of Joyce *et al.*, we believe that this type of structural transition has been experimentally observed.

(14) Chen, Y.-L.; Israelachvili, J. N. *J. Phys. Chem.* **1992**, *96*, 7752.